Follow us @BoneJointRes

Freely available online OPEN ACCESS

BJR

CARTILAGE

GDF11 inhibits abnormal adipogenesis of condylar chondrocytes in temporomandibular joint osteoarthritis

H. Wang,
Y. Shi,
F. He,
T. Ye,
S. Yu,
H. Miao,
Q. Liu,
M. Zhang

From The Fourth Military Medical University, Xi'an, China

Aims

Abnormal lipid metabolism is involved in the development of osteoarthritis (OA). Growth differentiation factor 11 (GDF11) is crucial in inhibiting the differentiation of bone marrow mesenchymal stem cells into adipocytes. However, whether GDF11 participates in the abnormal adipogenesis of chondrocytes in OA cartilage is still unclear.

Methods

Six-week-old female mice were subjected to unilateral anterior crossbite (UAC) to induce OA in the temporomandibular joint (TMJ). Histochemical staining, immunohistochemical staining (IHC), and quantitative real-time polymerase chain reaction (qRT-PCR) were performed. Primary condylar chondrocytes of rats were stimulated with fluid flow shear stress (FFSS) and collected for oil red staining, immunofluorescence staining, qRT-PCR, and immunoprecipitation analysis.

Results

Abnormal adipogenesis, characterized by increased expression of CCAAT/enhancer-binding protein α (CEBPα), fatty acid binding protein 4 (FABP4), Perilipin1, Adiponectin (AdipoQ), and peroxisome proliferator-activated receptor γ (PPARγ), was enhanced in the degenerative cartilage of TMJ OA in UAC mice, accompanied by decreased expression of GDF11. After FFSS stimulation, there were fat droplets in the cytoplasm of cultured cells with increased expression of PPARγ, CEBPα, FABP4, Perilipin1, and AdipoQ and decreased expression of GDF11. Exogenous GDF11 inhibited increased lipid droplets and expression of AdipoQ, CEBPα, and FABP4 induced by FFSS stimulation. GDF11 did not affect the change in PPARγ expression under FFSS, but promoted its post-translational modification by small ubiquitin-related modifier (SUMOylation). Local injection of GDF11 alleviated TMJ OA-related cartilage degeneration and abnormal adipogenesis in UAC mice.

Conclusion

Abnormal adipogenesis of chondrocytes and decreased GDF11 expression were observed in degenerative cartilage of TMJ OA. GDF11 supplementation effectively inhibits the adipogenesis of chondrocytes and thus alleviates TMJ condylar cartilage degeneration. GDF11 may inhibit the abnormal adipogenesis of chondrocytes by affecting the SUMOylation of PPARγ.

Cite this article: *Bone Joint Res* 2022;11(7):453–464.

Keywords: Temporomandibular joint, Osteoarthritis, Chondrocyte, SUMOylation, GDF11

Article focus

- Abnormal lipid formation, involved in the development of osteoarthritis (OA), could induce further damage of cartilage. However, the mechanism is still unclear.
- Growth differentiation factor 11 (GDF11) is the potential inhibitor of adipogenic process. Thus, the role of GDF11 in lipid formation in temporomandibular joint (TMJ) OA and its mechanism need further study.

Key messages

- Mice stimulated with unilateral anterior crossbite (UAC) presented with obvious cartilage degeneration in TMJ condylar cartilage, accompanied by decreased expression of GDF11 and increased

Correspondence should be sent to Mian Zhang; email: zhangmian1986@aliyun.com

doi: 10.1302/2046-3758.117.BJR-2022-0019.R1

Bone Joint Res 2022;11(7):453–464.

expression of adipogenic-related molecules. Supplementation of GDF11 reversed these changes.
- Primary chondrocytes from TMJ condylar cartilage, subjected to fluid flow shear stress (FFSS), expressed reduced GDF11 and enhanced adipogenic-related molecules.
- GDF11 inhibited lipid formation through the post-translational modification by small ubiquitin-related modifier (SUMOylation) of proliferator-activated receptor γ (PPARγ).

Strengths and limitations

- To our knowledge, this is the first time that the inhibitory role of GDF11 in lipid formation of chondrocytes through the induction of PPARγ SUMOylation has been disclosed. These findings could provide a new view on the understanding of OA.
- It is unfortunate that we were not able to verify our findings in human OA.

Introduction

Temporomandibular joint (TMJ) osteoarthritis (OA) is a severe manifestation of temporomandibular disorder (TMD), and 14.56% of TMD patients in mainland China show signs of TMJ OA by CT examination.[1,2] The degeneration of TMJ condylar cartilage is the main pathological change in TMJ OA.[3,4] Condylar chondrocytes, as the only cell type in TMJ condylar cartilage, play a decisive role in the process of cartilage degeneration, but the mechanism remains to be further clarified.[5,6] In recent years, studies have shown that abnormal lipid metabolism is involved in the development of knee OA, and obvious adipogenesis occurs in knee OA chondrocytes,[7-9] but whether there are similar changes in TMJ OA chondrocytes has not yet been reported. There are various molecules regulating the process of adipogenesis. Peroxisome proliferator-activated receptor γ (PPARγ) expresses early during adipogenesis, and is essential in the process of adipogenesis. CCAAT/enhancer-binding protein α (CEBPα) is then activated, which further promotes the expression of adipocyte-related genes, such as fatty acid binding protein 4 (FABP4), Perilipin1, and adiponectin (AdipoQ).[10,11]

Growth differentiation factor 11 (GDF11), a novel transforming growth factor-β (TGF-β) superfamily member, was shown to be crucial during the development and progression of multiple diseases.[12,13] Accumulating evidence indicates that GDF11 might be involved in adipogenesis. The expression of GDF11 was shown to decrease in the skeletal muscle of obese mice.[14,15] Moreover, in women older than 60 years of age, GDF11 was reported to be negatively correlated with body mass, BMI, and fat mass.[16] Recently, GDF11 has been found to inhibit the differentiation of bone marrow mesenchymal stem cells into adipocytes, and reduce lipid deposition in monocytes and liver cells.[17,18] Protein post-translational modification by small ubiquitin-related modifier (SUMO), termed SUMOylation, plays an essential role in a variety of cellular processes.[19] It has been reported that GDF11 could inhibit the activity of PPARγ by promoting its SUMOylation, which is associated with the decrease in adipogenesis of MSCs.[18] However, there is still a lack of research on the change in GDF11 expression in degenerative cartilage of TMJ OA and its impact on adipogenesis of chondrocytes.

In our previous studies, we induced TMJ OA lesions by applying unilateral anterior crossbite (UAC) stimulation to rodents. The condylar cartilage of rats and mice showed typical degenerative changes, such as decreased cartilage thickness, loss of matrix components, and increased OA score.[20-23] In this study, by applying UAC to mice to induce TMJ OA and fluid flow shear stress (FFSS) to primary rat condylar chondrocytes, the association between chondrocyte adipogenesis and GDF11 expression in TMJ condylar degenerative cartilage was clarified. Moreover, TMJ OA mice were locally injected with GDF11 in the TMJ area to explore the effect of GDF11 on the inhibition of chondrocyte adipogenesis and cartilage degeneration in the process of TMJ OA formation.

Methods

Animal group and tissue preparation. In total, 150 six-week-old C57BL/6 J female mice (17 to 19 g) were used in the study. The mice were divided into groups for sham group (n = 45), UAC groups (n = 45), and UAC with TMJ local injection groups (n = 60). The mice in the sham and UAC groups were further subdivided based on the following time points: three weeks (3 WK), seven weeks (7 WK), and 11 weeks (11 WK) (n = 15 in each subgroup), respectively. The mice in UAC with TMJ local injection groups were assigned into subgroups of 7 WK UAC with vehicle injection, 7 WK UAC with GDF11 injection, 11 WK UAC with vehicle injection, and 7 WK UAC with GDF11 injection.

The mice were killed according to the group timepoints by an overdose of pentobarbital, and the TMJs were obtained. There were no notable differences between the left and right TMJ samples in histomorphology or molecular properties. A total of 15 collected left TMJs from each group were randomly divided into three groups, and ten right TMJs were randomly divided into two groups for RNA extraction and further quantitative real-time polymerase chain reaction (qRT-PCR) analysis (n = 5). The remaining five TMJs from the right side were used for safranin O and immunohistochemical staining (IHC; n = 5).

UAC application. The UAC operation was performed as we described previously.[20,24,25] All animals were housed in a pathogen-free room and given sterilized food and distilled water during the study. The animals were housed at a density of no more than four animals in a single cage (measuring 50 × 40 × 25 cm) under an ambient temperature of 20°C (± 2°C), with a humidity of 55% (± 5%) and good ventilation and also 12 hr/12 hr dark/light cycles (4 W per square metre). The sterilized wood chip bedding was replaced every other day. Animal health status was monitored twice daily. All animals were healthy

Table I. Gene primer sequences for mouse used for quantitative real-time polymerase chain reaction.

Genes	Forward primers	Reverse primers
Adipoq	CCCCGGAACCCCTGGCAGGAAAG	GGGTCTCCAGCCCCACACTGAACG
Aggrecan	GGAGACCCAGACAGCAGAAACAAC	GCAGGTGGCTCCATTCAGACAAG
Alp	CCAGAAAGACACCTTGACTGTGG	TCTTGTCCGTGTCGCTCACCAT
Cebpα	TCGGTGGACAAGAACAGCAACG	CGGTCATTGTCACTGGTCAACTCC
Col-II	GGTCCTCCTGGTCCTGGCATC	CGTGCTGTCTCAAGGTACTGTCTG
Col-X	ATGCCGCTTGTCAGTGCTAACC	GGGTCGTAATGCTGCTGCCTATTG
Fabp4	CGCAGACGACAGGAAGGTGA	TCCACCACCAGCTTGTCACC
GAPDH	TGTGTCCGTCGTGGATCTGA	TTGCTGTTGAAGTCGCAGGAG
GDF11	GCGTCACATCCGTATCCGTTCAC	GCTCTGTGGCTGGCGAAACC
Mmp13	ACTTCACGATGGCATTGCTG	CATAATTTGGCCCAGGAGGA
Perilipin1	AACCCTGCTGGATGGAGACCTC	TGGGCTTCTTTGGTGCTGTTGTAG
PPARγ	GCCTGCGGAAGCCCTTTGGTGAC	TCAGCAAGCCTGGGCGGTCTCC

Alp, alkaline phosphatase; Cebpα, CCAAT/enhancer-binding protein α; Col-II, type II collagen; Col-X, type X collagen; Fabp4, fatty acid binding protein 4; GAPDH, glyceraldehyde-3-phosphate dehydrogenase; GDF11, growth differentiation factor 11; MMP13, matrix metalloproteinase 13; PPARγ, peroxisome proliferator-activated receptor gamma.

throughout the study. No adverse events other than TMJ pathology were observed. All animals were euthanized via overdose with a single intraperitoneal injection of pentobarbital sodium before tissue harvesting. We have included an ARRIVE checklist to show that we have conformed to the ARRIVE guidelines in this study. Two suitable metal tubes made of a pinhead were attached to the left maxillary and mandibular incisors separately under deep anaesthesia with intraperitoneal injection of 1% sodium pentobarbital. The tube for the mandibular incisors had a curved, 135°, labially inclined occlusal plate to create a crossbite relationship with the maxillary-tubed incisor. Mice in the sham groups received the same procedure but without the attachment of metal tubes.

TMJ local area injection. The TMJ local area injection was performed as we described previously.[20,24,25] Mice were anaesthetized using intraperitoneal injection of 1% sodium pentobarbital. The needle was inserted below the zygomatic arch between the eye and ear until it reached the outer surface of the mandibular ramus, after which it was adjusted to go along the bone and finally reach the TMJ region. Injections began on the second day of UAC operation and were administered to the UAC with TMJ injection groups every two days. GDF11 (10 μM, P6319, Abnova, USA) was injected to UAC with GDF11 injection groups and the same volume of vehicle to UAC with vehicle injection group.

Safranin O staining and immunohistochemical staining. TMJ blocks were fixed, decalcified, dehydrated, and embedded using conventional methods. The 5 μm thick sagittal sections were used for histomorphology and IHC. The serial sections were stained with Safranin O, in order to observe histological and proteoglycan changes in the articular cartilage. IHC with anti-AdipoQ antibody (ab22554, Abcam, USA), anti-PPARγ antibody (ab41928, Abcam), and anti-GDF11 antibody (ab124721, Abcam) was performed as a standard, three-step, avidin-biotin complex staining procedure. Images were captured by a Leica light microscope (Leica 2500, Leica, Germany).

Isolation and culture of primary chondrocyte. The cartilage was dissected carefully and digested in 0.25% trypsin (Hyclone, USA) for 20 minutes followed by 0.2% type II collagenase (Gibco, USA) for three hours. The isolated cells were re-suspended in Dulbecco's Modified Eagle Medium (DMEM) (Hyclone, USA) with 10% (v/v) fetal bovine serum (FBS) and 1% penicillin-streptomycin (Hyclone), and then cultured in a fully humidified atmosphere with 5% CO_2 at 37°C. The medium was replaced every two days, and the cells reached confluence and adherence in culture for further experiments.

FFSS treatment and adipogenic induction. Primary chondrocytes were isolated from the three-week-old female rat mandibular condylar cartilage as we previously described.[25,26] Primary chondrocytes were subjected to FFSS treatment at 0, 12, and 24 dyne/cm^2 using the Flexcell Streamer system (Flexcell, USA) as we recently reported.[26] After FFSS stimulation, the cells were cultured in adipogenic induction medium. FFSS was performed every week, and adipogenic induction continued for three weeks. According to the related results of adipogenesis experiments, we used 24 dyne/cm^2 FFSS stimulation in further studies in which we added vehicle, 5 μM GDF11, or 10 μM GDF11 to the medium. Oil red O staining and immunofluorescent staining were performed after induction. The cells were fixed with 4% paraformaldehyde for 30 minutes and rinsed with phosphate-buffered saline (PBS). For oil red O staining, the fixed cells were stained with oil red O (C0158, Beyotime, China) for ten minutes, rinsed with PBS three times, and observed under a light microscope. For immunofluorescent staining, the fixed cells were incubated with primary antibodies against AdipoQ, PPARγ, and GDF11 overnight at 4°C. Then, the cells were incubated with the Cy3 secondary antibody and stained with 4′,6-diamidino-2-phenylindole (DAPI). In addition, cells were collected to extract messenger RNA (mRNA) for further analysis.

qRT-PCR. The total RNA and protein were obtained from mice condylar cartilage and cultured cells using Tripure

Table II. Primer sequences for rat used for quantitative real-time polymerase chain reaction.

Genes	Forward primers	Reverse primers
Adipoq	GCCGTGATGGCAGAGATGGCACTC	TGGCCCTTCCGCTCCTGTCATTCC
Aggrecan	TGGCATTGAGGACAGCGAAG	TCCAGTGTGTAGCGTGTGGAAATAG
Alp	AGGAGGGAGTCGTTCATGGAGTG	ACCAGTGGCAGCAGCAATGTTC
Cebpα	AGTCGGTGGATAAGAACAGCAACG	CGGTCATTGTCACTGGTCAACTCC
Col-II	CAGCCAAGCAGTCATACC	GTCACCTCTGGGTCCTTGTTCAC
Col-X	CAGCCAAGCAGTCATACC	AGTGCTGCTGCCTGTTGT
Fabp4	GCTTCGCCACCAGGAAAGTG	TCATCGAATTCCACGCCCAGT
GAPDH	GGCACAGTCAAGGCTGAGAATG	ATGGTGGTGAAGACGCCAGTA
GDF11	GGACTGGATCATCGCACCTAAGC	AGCAGAGCCTCGTGGGTTGG
Mmp13	ACTTCACGATGGCATTGCTG	CATAATTTGGCCCAGGAGGA
Perilipin1	GCCCGACCCTGCTGGATGGAGAC	ACTCACAGGTCCCGCTCACCACAG
PPARγ	GCCTGCGGAAGCCCTTTGGTGAC	TCAGCAAGCCTGGGCGGTCTCC

Alp, alkaline phosphatase; Cebpα, CCAAT/enhancer-binding protein α; Col-II, type II collagen; Col-X, type X collagen; Fabp4, fatty acid binding protein 4; GAPDH, glyceraldehyde-3-phosphate dehydrogenase; GDF11, growth differentiation factor 11; Mmp13, matrix metallopeptidase 13; PPARγ, peroxisome proliferator-activated receptor gamma.

(Roche, USA) according to the manufacturer's instructions. RNA of each sample was reverse transcribed to complementary DNA (cDNA) utilizing PrimeScript RT Reagent Kit Perfect Real Time (RR036A, TaKaRa Biotechnology, Japan). The cDNA was then used as a template to perform PCR on CFX Connect Real-Time System (Bio-Rad, USA). The amount of target mRNA was calculated using the formula $2^{-\Delta\Delta CT}$. The primers used for mice and rats are shown in Tables I and II, respectively.

Immunoprecipitation and western blot analysis. Cell lysates were precleared with 30 µl of Dynabeads Protein A (Invitrogen, USA), BSA, and related immunoglobulin G (IgG) antibody (Santa Cruz Biotechnology, USA) for three hours at 4°C, and then subjected to immunoprecipitation with antibodies against IgG, PPARγ, and SUMO-1 overnight at 4°C. Next, 50 µl Dynabeads Protein A were added, and the samples were incubated overnight at 4°C. Finally, the immunoprecipitates were washed with lysis buffer five times. The samples were then boiled for five minutes. Total proteins and immunoprecipitates were applied to sodium dodecyl sulfate (SDS)–polyacrylamide gels. After electrophoresis, the proteins were transferred to polyvinylidene fluoride (PVDF) membranes, followed by blocking in buffer containing 5% fat-free dry milk. The membranes were then probed with the indicated anti-β-actin (AF7018, Affinity, USA), anti-PPARγ, and anti-SUMO-1 (ab32058, Abcam) antibodies overnight, washed, incubated with HRP-conjugated secondary antibodies for 1.5 hours, and finally visualized using chemiluminescent enhanced chemiluminescence reagent (Vigorous Biotechnology, China).

Statistical analysis. All the data were retrieved from independent samples or observations. Statistics were analyzed using Graphpad Prism 7 software (GraphPad Software, USA). Data are presented as the means (standard errors) for each group. The normality of the data distribution was tested using the Shapiro-Wilk test with 95% confidence, and Levene's test was used to assess homogeneity of variance. For two compared groups, statistical significance was evaluated by independent-samples *t*-test if the homogeneity of variance was consistent, or evaluated by Satterthwaite's *t*-test if the homogeneity of variance was not equal. For three compared groups, one-way analysis of variance (ANOVA) was used to analyze the significance in groups. If the one-way ANOVA was statistically significant, Dunnett's method was used to evaluate the statistical significance in all pairwise comparisons if the homogeneity of variance was consistent. If the homogeneity of variance was not equal, Dunnett's T3 method was used to evaluate the statistical significance in all pairwise comparisons. The statistical significance was defined as $p < 0.05$.

Results

Abnormal adipogenesis was observed in the degenerated condylar cartilage of TMJ OA. In the TMJ condylar cartilage of control mice, the prehypertrophic and hypertrophic zones were positive for safranin O staining, suggesting that there was more proteoglycan in the cartilage matrix. The thickness of condylar cartilage (3 WK: $p = 0.024$; 7 WK: $p = 0.005$; 11 WK: $p < 0.001$) and the positive safranin O staining area (3 WK: $p = 0.002$; 7 WK: $p < 0.001$; 11 WK: $p < 0.001$, all independent-samples *t*-test) were significantly decreased in mice of the UAC groups, indicative of degenerative cartilage in the TMJ (Figures 1a and 1b). qRT-PCR also showed that the mRNA expression of type II collagen (*Col-II*; 7 WK: $p = 0.016$; 11 WK: $p < 0.001$) and *Aggrecan* (7 WK: $p < 0.001$; 11 WK: $p < 0.001$, all independent-samples *t*-test) was significantly lower in the condylar cartilage of mice in the UAC groups than in the control groups. The mRNA expression of markers of chondrocyte differentiation, such as type X collagen (*Col-X*; 3 WK: $p = 0.003$; 7 WK: $p < 0.001$; 11 WK: $p < 0.001$), alkaline phosphatase (*Alp*; 3 WK: $p = 0.010$; 7 WK: $p = 0.005$; 11 WK: $p = 0.001$), and matrix metallopeptidase 13 (*Mmp13*; 3 WK: $p = 0.003$; 7 WK: $p < 0.001$; 11 WK: $p = 0.001$, all independent-samples *t*-test) was significantly increased in the UAC groups (Figure 1c). In addition, the

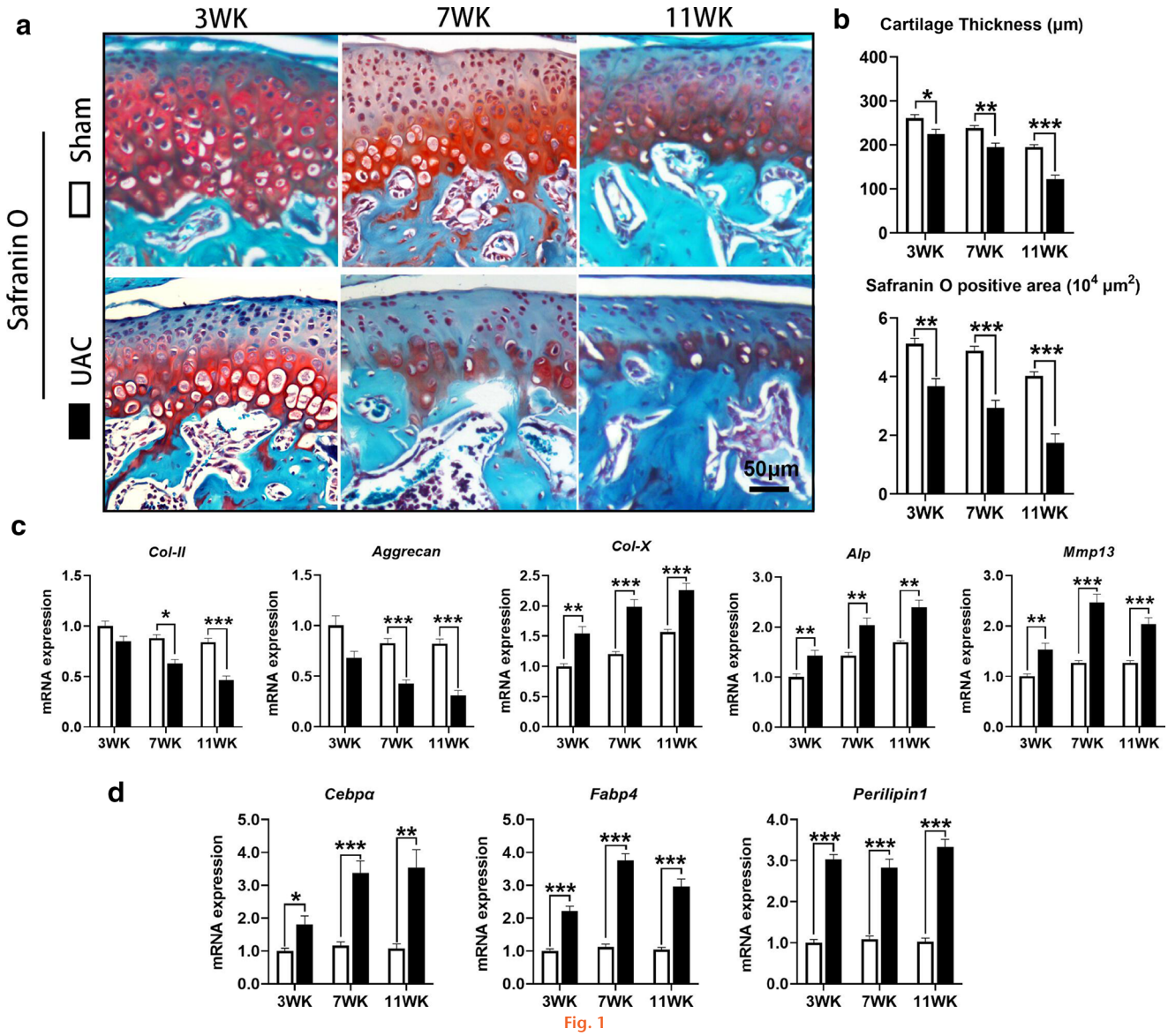

Fig. 1

Degeneration of condylar cartilage in mice with temporomandibular joint (TMJ) osteoarthritis (OA) induced by unilateral anterior crossbite (UAC) stimulation. a) Cartilage degeneration was obvious in the TMJs of UAC mice. b) The thickness of the condylar cartilage and safranin O positive area were significantly decreased in the TMJs of UAC mice. c) The messenger RNA (mRNA) expression of type II collagen (*Col-II*) and *Aggrecan* was decreased in the TMJs of UAC mice, accompanied by increased mRNA expression of type X collagen (*Col-X*), alkaline phosphatase (*Alp*), and matrix metallopeptidase 13 (*Mmp13*). d) The mRNA expression of CCAAT/enhancer-binding protein α (*Cebpα*), fatty acid binding protein 4 (*Fabp4*), and *Perilipin1* was increased in the TMJs of UAC mice. Sham, sham group; 3 WK, 3 weeks; 7 WK, 7 weeks; 11 WK, 11 weeks. *p < 0.05, **p < 0.01, ***p < 0.001 compared with the age-matched sham group, independent-samples *t*-test.

mRNA expression of three key markers of adipogenesis, *Cebpα* (3 WK: p = 0.018; 7 WK: p < 0.001; 11 WK: p = 0.002), *Fabp4* (3 WK: p < 0.001; 7 WK: p < 0.001; 11 WK: p < 0.001), and *Perilipin1* (3 WK: p < 0.001; 7 WK: p < 0.001; 11 WK: p < 0.001, all independent-samples *t*-test) was also significantly increased in UAC mice (Figure 1d).

IHC showed that the number of AdipoQ-positive chondrocytes in the condylar cartilage of the control group was very small, while the number of AdipoQ-positive chondrocytes in the condylar cartilage of the UAC group was significantly increased (3 WK: p < 0.001; 7 WK: p < 0.001; 11 WK: p < 0.001), and the mRNA expression of *Adipoq* (3 WK: p < 0.001; 7 WK: p < 0.001; 11 WK: p < 0.001, all independent-samples *t*-test) was also significantly elevated in UAC mice (Figures 2a and 2b). The number of PPARγ-positive cells in the condylar cartilage of the control mice was lower, while the number of PPARγ-positive cells in the condylar cartilage of the UAC mice was significantly increased (3 WK: p < 0.001; 7 WK: p < 0.001; 11 WK: p < 0.001), and mRNA expression of *PPARγ* was also significantly upregulated (3 WK: p = 0.003; 7 WK: p < 0.001; 11 WK: p < 0.001, all independent-samples *t*-test) (Figures 2c and 2d).

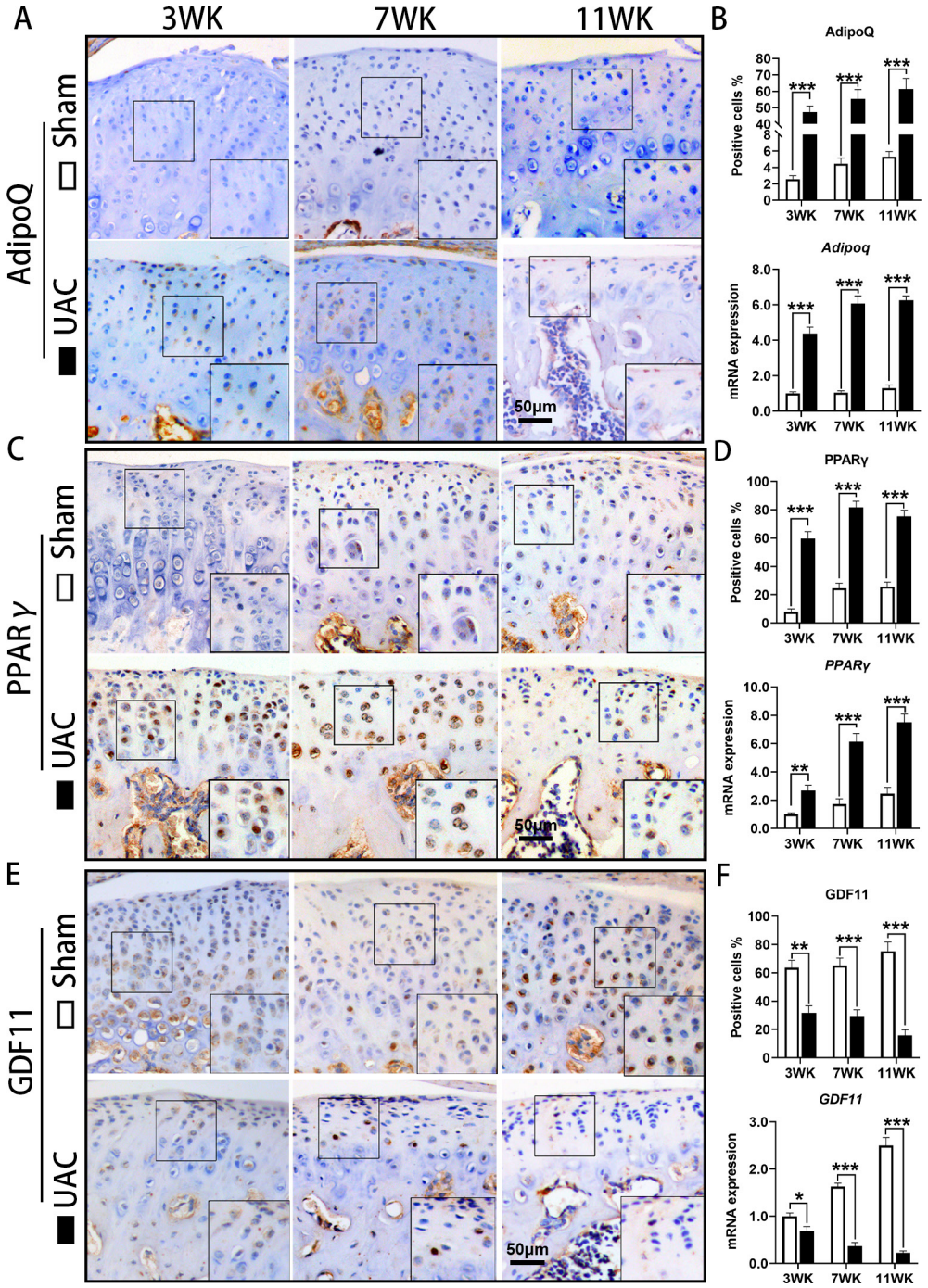

Fig. 2

Abnormal adipogenesis in condylar cartilage of mice with temporomandibular joint (TMJ) osteoarthritis (OA) induced by unilateral anterior crossbite (UAC) stimulation. a) Immunohistochemical staining (IHC) of Adiponectin (AdipoQ) in the TMJs of sham and UAC mice. b) The proportion of AdipoQ-positive chondrocytes and messenger RNA (mRNA) expression of *AdipoQ* were increased in the TMJs of UAC mice. c) IHC of peroxisome proliferator-activated receptor γ (PPARγ) in the TMJs of sham and UAC mice. d) The proportion of PPARγ-positive chondrocytes and mRNA expression of *PPARγ* were increased in the TMJs of UAC mice. e) IHC of growth differentiation factor 11 (GDF11) in the TMJs of sham and UAC mice. f) The proportion of GDF11-positive chondrocytes and mRNA expression of *GDF11* were decreased in the TMJs of UAC mice. Sham, sham group; 3 WK, 3 weeks; 7 WK, 7 weeks; 11 WK, 11 weeks. *p < 0.05, **p < 0.01, ***p < 0.001 compared with the age-matched sham group, independent-samples *t*-test .

The expression of GDF11 decreased in the condylar cartilage of TMJ OA mice. IHC showed that GDF11 was widely expressed in TMJ condylar cartilage of control mice, while GDF11-positive cell numbers were significantly decreased in the UAC groups (3 WK: p = 0.002; 7 WK: p = 0.001; 11 WK: p < 0.001), and the mRNA expression level of *GDF11* in the condylar cartilage of mice in the UAC

groups was also significantly higher than that in the control groups (3 WK: $p = 0.011$; 7 WK: $p < 0.001$; 11 WK: $p < 0.001$, all independent-samples *t*-test) (Figures 2e and 2f).

FFSS promoted abnormal adipogenesis and inhibited GDF11 expression in primary condylar chondrocytes. Different degrees of FFSS were applied to primary rat TMJ condylar chondrocytes for three times which were cultured in adipogenic induction medium for 21 days, and qRT-PCR examination showed that the mRNA expression of *Col-II* (12 dyne/cm^2: $p = 0.027$; 24 dyne/cm^2: $p = 0.006$) and *Aggrecan* (12 dyne/cm^2: $p = 0.045$; 24 dyne/cm^2: $p = 0.001$) was significantly decreased, while the mRNA expression level of the differentiation markers *Col-X* (12 dyne/cm^2: $p = 0.034$; 24 dyne/cm^2: $p < 0.001$), *Alp*(12 dyne/cm^2: $p = 0.048$; 24 dyne/cm^2: $p = 0.001$), and *Mmp13* (12 dyne/cm^2: $p = 0.037$; 24 dyne/cm^2: $p < 0.001$, all one-way ANOVA) was significantly increased (Figure 3a), suggesting that FFSS can induce the degeneration and differentiation of condyle chondrocytes.

At the same time, qRT-PCR also demonstrated that the mRNA expression of *PPARγ* (12 dyne/cm^2: $p = 0.045$; 24 dyne/cm^2: $p < 0.001$), *Cebpα* (12 dyne/cm^2: $p = 0.036$; 24 dyne/cm^2: $p < 0.001$), *Fabp4* (12 dyne/cm^2: $p = 0.049$; 24 dyne/cm^2: $p < 0.001$), *Perilipin1* (12 dyne/cm^2: $p = 0.049$; 24 dyne/cm^2: $p = 0.001$), and *Adipoq* (12 dyne/cm^2: $p = 0.050$; 24 dyne/cm^2: $p < 0.001$, all one-way ANOVA) was significantly increased after FFSS stimulation (Figure 3a). Oil red O staining showed that no obvious lipid droplets existed in cultured condylar chondrocytes of the control group (0 dyne/cm^2), while after FFSS stimulation fat droplets were clearly observed in condylar chondrocytes (Figure 3b), also suggesting that FFSS can induce abnormal adipogenesis of chondrocytes. Immunofluorescence staining confirmed that the expression of AdipoQ (12 dyne/cm^2: $p = 0.034$; 24 dyne/cm^2: $p < 0.001$) and PPARγ (12 dyne/cm^2: $p = 0.038$; 24 dyne/cm^2: $p = 0.006$, all one-way ANOVA) was low in the cytoplasm of condylar chondrocytes in the control group (0 dyne/cm^2), and was significantly increased after FFSS stimulation (Figure 3c).

In contrast to the increased abnormal adipogenesis results, GDF11 was more highly expressed in the cytoplasm of condylar chondrocytes in the control group, while after FFSS stimulation the expression of GDF11 in the cytoplasm was significantly decreased (12 dyne/cm^2: $p = 0.015$; 24 dyne/cm^2: $p = 0.001$) (Figure 3d), and its mRNA expression was also significantly downregulated (12 dyne/cm^2: $p = 0.021$; 24 dyne/cm^2: $p = 0.001$, all one-way ANOVA) (Figure 3e). Western blot assays showed that FFSS increased PPARγ protein content in condylar chondrocytes and decreased its SUMOylation (Figure 3f).

Exogenous GDF11 inhibited FFSS-induced abnormal adipogenesis of condylar chondrocytes. According to the above results, 24 dyne/cm^2 was selected in further experiments with FFSS stimulation, and different concentrations of exogenous GDF11 were added in condylar chondrocytes to explore the inhibitory effect of GDF11 on adipogenesis. qRT-PCR results in condylar chondrocytes showed that after the addition of GDF11, the FFSS-induced changes in the mRNA expression of markers, such as *Col-II* (10 μM GDF11: $p = 0.001$), *Aggrecan* (10 μM GDF11: $p < 0.001$), *Col-X* (5 μM GDF11: $p = 0.021$; 10 μM GDF11: $p = 0.002$), *Alp* (10 μM GDF11: $p = 0.004$), and *Mmp13* (5 μM GDF11: $p = 0.046$; 10 μM GDF11: $p = 0.001$, all one-way ANOVA) were all reversed in a dose-dependent manner (Figure 4a).

Moreover, the FFSS-stimulated increases in the mRNA expression of *Cebpα* (10 μM GDF11: $p = 0.014$), *Fabp4* (5 μM GDF11: $p = 0.038$; 10 μM GDF11: $p = 0.001$), *Perilipin1* (5 μM GDF11: $p = 0.009$; 10 μM GDF11: $p = 0.005$), and *Adipoq* (10 μM GDF11: $p < 0.001$, all one-way ANOVA) were significantly decreased after the addition of GDF11 in a dose-dependent manner (Figure 4a). However, exogenous GDF11 had no significant effect on the FFSS-induced upregulation of *PPARγ* mRNA expression (Figure 4a).

Oil red O staining showed that exogenous GDF11 significantly reduced the fat droplets produced by FFSS stimulation in condylar chondrocytes (Figure 4c). At the same time, the significant increase in AdipoQ expression in the cytoplasm of condylar chondrocytes after FFSS stimulation was also significantly reversed by the addition of GDF11 (5 μM GDF11: $p = 0.017$; 10 μM GDF11: $p = 0.002$, one-way ANOVA) (Figure 4b). However, the addition of exogenous GDF11 had no effect on the increase in PPARγ expression in the cytoplasm (Figure 4b). Western blot assays showed that GDF11 did not reduce the increased PPARγ protein content in condylar chondrocytes after FFSS stimulation, but GDF11 significantly promoted the SUMOylation of PPARγ (Figure 4d), thereby reducing the effect of PPARγ on adipogenesis.

Local injection of GDF11 inhibited condylar cartilage degeneration and abnormal lipid formation in UAC mice. TMJ injection of GDF11 into UAC mice showed that compared with that in the vehicle-injected UAC group, the positive safranin O staining area was significantly increased (7 WK: $p = 0.014$; 11 WK: $p = 0.001$, independent-samples *t*-test), suggesting increased proteoglycan content in the cartilage matrix. Moreover, the thickness of condylar cartilage in the UAC groups injected with GDF11 was significantly increased (7 WK: $p = 0.020$; 11 WK: $p = 0.018$, independent-samples *t*-test) (Figures 5a and 5b).

IHC showed that the number of AdipoQ-positive chondrocytes in the condylar cartilage of mice in the UAC groups was significantly decreased after GDF11 injection (7 WK: $p < 0.001$; 11 WK: $p < 0.001$), and the mRNA expression of *Adipoq* (7 WK: $p = 0.002$; 11 WK: $p = 0.002$, all independent-samples *t*-test) was also significantly decreased. However, local injection of GDF11 had no significant effect on the increase in the number of PPARγ-positive cells or the upregulation of mRNA expression in mouse condylar cartilage induced by UAC stimulation (Figures 5c and 5d).

qRT-PCR assay showed that after GDF11 injection, the mRNA expression of *Col-II* (7 WK: $p = 0.040$; 11 WK: $p < 0.001$) and Aggrecan (7 WK: $p = 0.012$; 11 WK: $p = 0.001$, all independent-samples *t*-test) significantly increased in condylar chondrocytes. The mRNA expression of *Col-X*

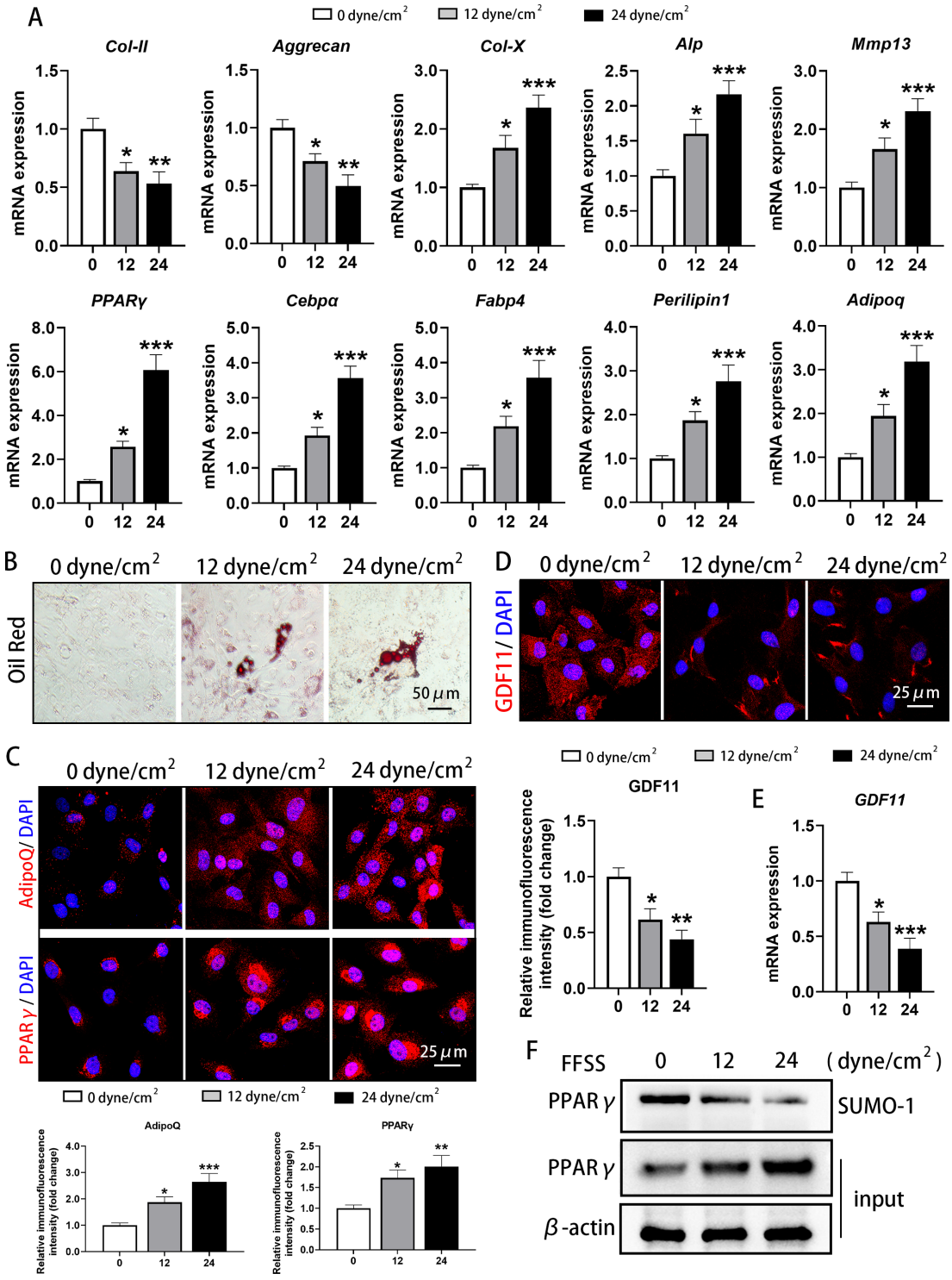

Fig. 3

Fluid flow shear stress (FFSS) promoted abnormal adipogenesis in cultured condylar chondrocytes and decreased the expression of growth differentiation factor 11 (GDF11). a) FFSS decreased the messenger RNA (mRNA) expression of type II collagen (*Col-II*) and aggrecan and increased expression of type X collagen (*Col-X*), alkaline phosphatase (*Alp*), matrix metallopeptidase 13 (*Mmp13*), peroxisome proliferator-activated receptor γ (*PPARγ*), CCAAT/enhancer-binding protein α (*Cebpα*), fatty acid binding protein 4 (*Fabp4*), *Perilipin1*, and Adiponectin (*Adipoq*) under adipogenic induction medium for 21 days. b) FFSS promoted the formation of lipid droplets in cultured condylar chondrocytes under adipogenic induction medium for 21 days. c) FFSS promoted the protein levels of AdipoQ and PPARγ in the cytoplasm of cultured condylar chondrocytes when cultured in adipogenic induction medium for 21 days. d) and e) FFSS decreased the d) protein level and e) mRNA expression of *GDF11* in the cytoplasm of cultured condylar chondrocytes when cultured in adipogenic induction medium for 21 days. f) FFSS induced the increase of PPARγ protein and the decrease of its post-translational modification by small ubiquitin-related modifier (SUMOylation) in cultured condylar chondrocytes when cultured in adipogenic induction medium for 21 days. *p < 0.05, **p < 0.01, ***p < 0.001 compared with the 0 dyne/cm^2 group, one-way analysis of variance (ANOVA). DAPI, 4′,6-diamidino-2-phenylindole; SUMO, small ubiquitin-related modifier.

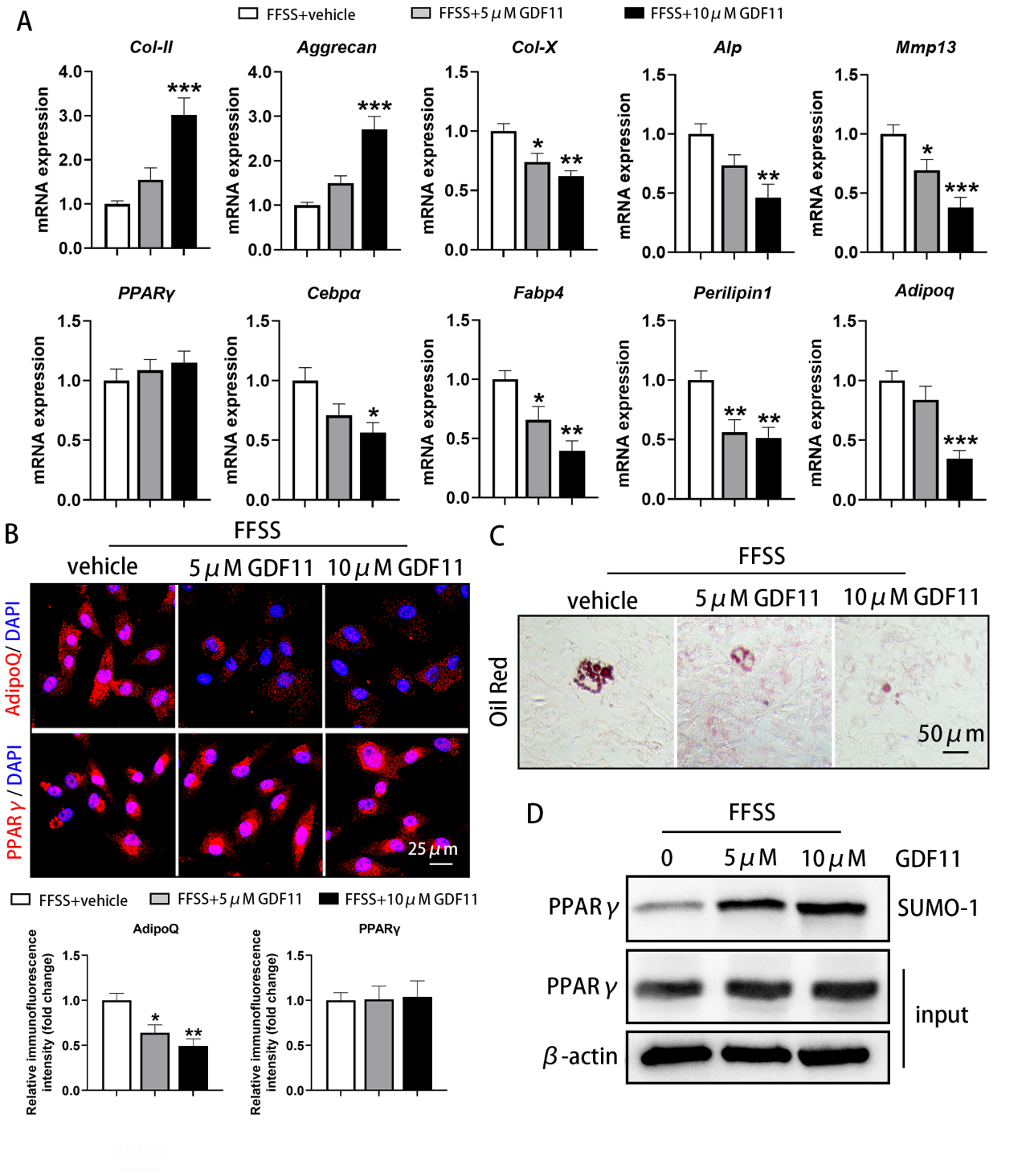

Fig. 4

Exogenous growth differentiation factor 11 (GDF11) alleviated the abnormal adipogenesis and differentiation of condylar chondrocytes induced by fluid flow shear stress (FFSS). a) Exogenous GDF11 increased the messenger RNA (mRNA) expression of type II collagen (*Col-II*) and *Aggrecan*, and decreased the mRNA expression of type X collagen (*Col-X*), alkaline phosphatase (*ALP*), matrix metallopeptidase 13 (*Mmp13*), CCAAT/enhancer-binding protein α (Cebpα), fatty acid binding protein 4 (*Fabp4*), *Perilipin1*, and Adiponectin (*Adipoq*) after FFSS stimulation in condylar chondrocytes when cultured in adipogenic induction medium for 21 days. However, it did not affect the changes in peroxisome proliferator-activated receptor γ (*PPARγ*) expression induced by FFSS. b) Exogenous GDF11 decreased the protein level of AdipoQ but had no influence on PPARγ expression in the cytoplasm of cultured condylar chondrocytes with adipogenic induction medium after FFSS stimulation. c) Exogenous GDF11 inhibited the enhanced formation of lipid droplets induced by FFSS in cultured condylar chondrocytes under adipogenic induction medium for 21 days. d) Exogenous GDF11 did not affect the FFSS-induced increase in PPARγ levels in the cytoplasm of cultured condylar chondrocytes, but it did significantly promote the post-translational modification by small ubiquitin-related modifier (SUMOylation) of PPARγ in chondrocytes when cultured in adipogenic induction medium for 21 days. *p < 0.05, **p < 0.01, ***p < 0.001 compared with the FFSS + vehicle group, one-way analysis of variance (ANOVA). DAPI, 4′,6-diamidino-2-phenylindole; SUMO, small ubiquitin-related modifier.

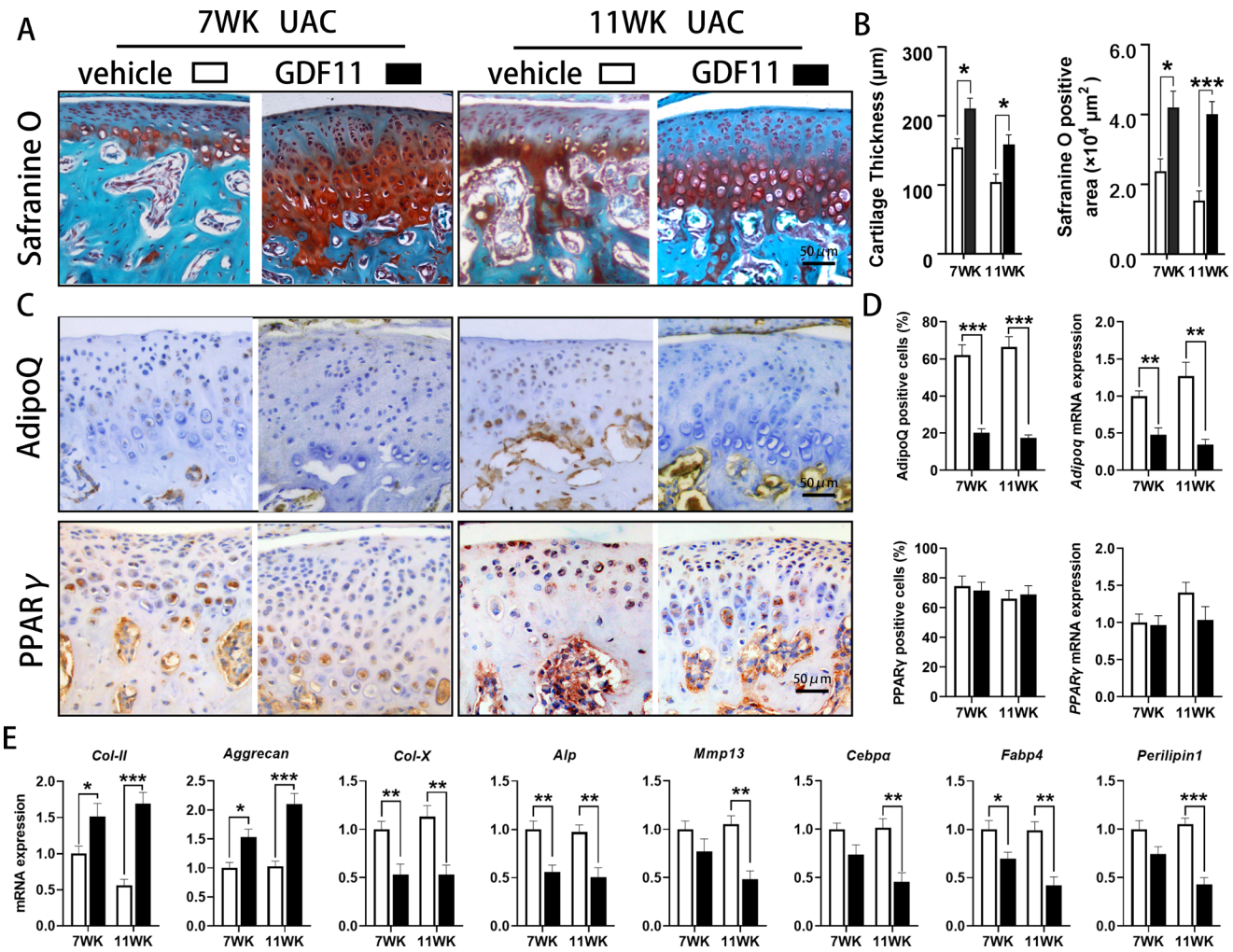

Fig. 5

Effect of local injection of growth differentiation factor 11 (GDF11) on cartilage degeneration and abnormal adipogenesis of condylar cartilage in the temporomandibular joints (TMJs) of mice. a) Cartilage degeneration of the TMJ was alleviated in unilateral anterior crossbite (UAC) mice injected with GDF11. b) The thickness of the condylar cartilage and safranine O positive area were significantly increased in the TMJs of UAC mice injected with GDF11. c) Immunohistochemical staining of Adiponectin (AdipoQ) and peroxisome proliferator-activated receptor γ (PPARγ) in the TMJs of UAC + vehicle-injected and UAC + GDF11-injected mice. d) The proportion of AdipoQ-positive chondrocytes and messenger RNA (mRNA) expression of *Adipo*q were decreased in the TMJs of UAC mice injected with GDF11. However, GDF11 injection did not affect the change in PPARγ in the TMJs of mice under UAC stimulation. e) GDF11 injection increased the mRNA expression of type II collagen (*Col-II*) and *Aggrecan*, and decreased the mRNA expression of type X collagen (*Col-X*), alkaline phosphatase (Alp), matrix metallopeptidase 13 (*Mmp13*), *Adipoq*, CCAAT/enhancer-binding protein α (*Cebpa*), fatty acid binding protein 4 (*Fabp4*), and *Perilipin1* in the TMJs of UAC mice. Vehicle, vehicle injection group; GDF11, GDF11 injection group; 7 WK, 7 weeks; 11 WK, 11 weeks. *p < 0.05, **p < 0.01, ***p < 0.001 compared with the age-matched UAC + vehicle injection group, independent-samples *t*-test .

(7 WK: p = 0.009; 11 WK: p = 0.004), *Alp* (7 WK: p = 0.005; 11 WK: p = 0.005), *Mmp13* (11 WK: p = 0.002), *Cebpα* (11 WK: p = 0.003), *Fabp4* (7 WK: p = 0.027; 11 WK: p = 0.002), and *Perilipin1* (11 WK: p < 0.001, all independent-samples *t*-test) was significantly decreased (Figure 5e).

Discussion

TMJ OA is a severe manifestation of TMD, and the main pathological change is the degeneration of TMJ condylar cartilage.[3] However, the pathogenic factors of TMJ OA have not been fully defined at present. Abnormal biomechanical force stimulation plays a key role in the pathogenesis of OA of most joints, such as the knee and hip joints.[27-30] The TMJ is subjected to biological force stimulation when exercising masticatory function, and abnormal occlusion may lead to changes in the biomechanical environment to which the TMJ is subjected, inducing TMD and even TMJ OA.[31-33] In this study, we successfully induced osteoarthritic cartilage degeneration in the TMJ by constructing UAC to change the biomechanical environment of the TMJ in mice, which confirmed the key role of occlusal abnormalities in the pathogenesis of TMD and TMJ OA.

The main pathological change in OA is degeneration of cartilage tissue, and chondrocytes, as the only cell type in cartilage tissue, play a key role in maintaining cartilage homeostasis.[5,34] The abnormal function and activity of chondrocytes inevitably affects the health of the entire

joint.[5,6] Recent studies have found an important correlation between chondrocyte lipid metabolism and the incidence of OA.[35-37] Abnormal lipid metabolism leads to fatty disorders such as fat accumulation in chondrocytes, and the degree of fatty degeneration is positively correlated with the severity of OA.[35,38] In this study, there was no obvious adipogenesis in TMJ condylar cartilage of control mice, but the expression levels of the adipogenic markers CEBPα, FABP4, Perilipin1, and AdipoQ were markedly increased in condylar cartilage of TMJ OA mice, indicating abnormal adipogenesis in the process of TMJ OA formation, and the degree of abnormal adipogenesis also increased accordingly with the severity of TMJ OA. In vitro experiments confirmed that adipogenesis was clearly observed in chondrocytes after FFSS stimulation. Abnormal biomechanical force stimulation was determined as one of the reasons for the occurrence of adipogenesis.

GDF11 has been proven to inhibit the differentiation of bone marrow mesenchymal stem cells into adipocytes and can also inhibit lipid deposition in monocytes and hepatocytes,[17,39,40] so it has a clear anti-adipogenic effect. In this study, GDF11 was widely and highly expressed throughout the TMJ condylar cartilage of control mice, while the expression of GDF11 was greatly decreased in TMJ OA cartilage, suggesting that the reduction in GDF11 expression may be an important cause of chondrocyte adipogenesis in TMJ OA. In vitro experiments confirmed that supplementation with exogenous GDF11 substantially reduced FFSS-induced adipogenesis in chondrocytes. To further clarify the effect of GDF11, TMJ OA mice received a local injection of exogenous GDF11. The thickness of TMJ condylar cartilage and the matrix content were notably increased, accompanied by greatly inhibited adipogenesis in chondrocytes, indicating that GDF11 might play a role in inhibiting abnormal adipogenesis and degeneration in cartilage and be a new target for the treatment of TMJ OA. Similar to our results, it has been reported that GDF11 can markedly reduce age-related degeneration of knee cartilage in elderly mice,[41,42] which also suggests a positive protective effect of GDF11 on articular cartilage.

PPARγ is the convergence point of almost all adipogenesis signalling pathways, and the loss of PPARγ protein leads to the breakdown of almost all adipogenesis pathways.[43,44] Upregulation of PPARγ expression can induce increased adipogenic differentiation of bone marrow mesenchymal stem cells, leading to proliferation of adipose tissue in the bone marrow.[45] However, inhibiting the transcriptional activity of PPARγ can constrain the adipogenic differentiation of bone marrow mesenchymal stem cells.[46] In the condylar cartilage of TMJ OA mice, the expression of PPARγ was upregulated, and it was also substantially increased after FFSS stimulation. In vivo and in vitro experiments showed that PPARγ played a key role in the abnormal adipogenesis of chondrocytes induced by abnormal biomechanical forces. In vitro experiments showed that GDF11 greatly inhibited the abnormal adipogenesis of chondrocytes, but it had no notable effect on the expression of PPARγ. Therefore, PPARγ may be regulated in other ways. Our results confirmed that GDF11 can substantially promote the SUMOylation of PPARγ and thus affect the biological function of PPARγ, but its specific regulatory mechanism needs to be further studied. Moreover, the increased expression of PPARγ under UAC stimulation in vivo and FFSS stimulation in vitro might not be exclusively due to the decreased expression of GDF11. It seems that the inhibitory effect of GDF11 on adipogenesis is achieved by promoting SUMOylation of PPARγ, rather than directly affecting the expression of PPARγ. The reason for increased expression of PPARγ in cartilage of TMJ OA in mice remained unclear, which requires further study.

In conclusion, abnormal occlusion can induce OA lesions in TMJ condylar cartilage. There is extensive abnormal adipogenesis of chondrocytes in TMJ OA condylar degenerative cartilage. Supplementation with exogenous GDF11 can effectively inhibit the adipogenesis of chondrocytes and thus alleviate the degree of degeneration of condylar cartilage. GDF11 may inhibit the abnormal adipogenesis of chondrocytes by affecting the SUMOylation of PPARγ, but the specific mechanism still needs to be further studied.

Supplementary material

An ARRIVE checklist is included to show that the ARRIVE guidelines were adhered to in this study.

References

1. **Pantoja LLQ**, **de Toledo IP**, **Pupo YM**, **et al**. Prevalence of degenerative joint disease of the temporomandibular joint: a systematic review. *Clin Oral Investig*. 2019;23(5):2475–2488.
2. **Zhao Y**, **Zhang Z**, **Wu Y**, **Zhang W**, **Ma X**. Investigation of the clinical and radiographic features of osteoarthrosis of the temporomandibular joints in adolescents and young adults. *Oral Surg Oral Med Oral Pathol Oral Radiol Endod*. 2011;111(2):e27-34.
3. **Liu Q**, **Yang H**, **Zhang M**, **et al**. Initiation and progression of dental-stimulated temporomandibular joints osteoarthritis. *Osteoarthr Cartil*. 2021;29(5):633–642.
4. **Charlier E**, **Deroyer C**, **Ciregia F**, **et al**. Chondrocyte dedifferentiation and osteoarthritis (OA). *Biochem Pharmacol*. 2019;165:49–65.
5. **Rim YA**, **Nam Y**, **Ju JH**. The role of chondrocyte hypertrophy and senescence in osteoarthritis initiation and progression. *Int J Mol Sci*. 2020;21(7):E2358.
6. **Zheng L**, **Zhang Z**, **Sheng P**, **Mobasheri A**. The role of metabolism in chondrocyte dysfunction and the progression of osteoarthritis. *Ageing Res Rev*. 2021;66:101249.
7. **Valdes AM**, **Ravipati S**, **Pousinis P**, **et al**. Omega-6 oxylipins generated by soluble epoxide hydrolase are associated with knee osteoarthritis. *J Lipid Res*. 2018;59(9):1763–1770.
8. **Jónasdóttir HS**, **Brouwers H**, **Kwekkeboom JC**, **et al**. Targeted lipidomics reveals activation of resolution pathways in knee osteoarthritis in humans. *Osteoarthr Cartil*. 2017;25(7):1150–1160.
9. **Korostynski M**, **Malek N**, **Piechota M**, **Starowicz K**. Cell-type-specific gene expression patterns in the knee cartilage in an osteoarthritis rat model. *Funct Integr Genomics*. 2018;18(1):79–87.
10. **Gregoire FM**, **Smas CM**, **Sul HS**. Understanding adipocyte differentiation. *Physiol Rev*. 1998;78(3):783–809.
11. **Cristancho AG**, **Lazar MA**. Forming functional fat: a growing understanding of adipocyte differentiation. *Nat Rev Mol Cell Biol*. 2011;12(11):722–734.
12. **Loffredo FS**, **Steinhauser ML**, **Jay SM**, **et al**. Growth differentiation factor 11 is a circulating factor that reverses age-related cardiac hypertrophy. *Cell*. 2013;153(4):828–839.

13. **Walker RG**, **Poggioli T**, **Katsimpardi L**, **et al**. Biochemistry and biology of GDF11 and myostatin: similarities, differences, and questions for future investigation. *Circ Res*. 2016;118(7):1125–1141.
14. **Jing YY**, **Li D**, **Wu F**, **Gong LL**, **Li R**. GDF11 does not improve the palmitate induced insulin resistance in C2C12. *Eur Rev Med Pharmacol Sci*. 2017;21(8):1795–1802.
15. **Egerman MA**, **Cadena SM**, **Gilbert JA**, **et al**. GDF11 increases with age and inhibits skeletal muscle regeneration. *Cell Metab*. 2015;22(1):164–174.
16. **Fife E**, **Kostka J**, **Kroc Ł**, **et al**. Relationship of muscle function to circulating myostatin, follistatin and GDF11 in older women and men. *BMC Geriatr*. 2018;18(1):200.
17. **Luo H**, **Guo Y**, **Liu Y**, **et al**. Growth differentiation factor 11 inhibits adipogenic differentiation by activating TGF-beta/Smad signalling pathway. *Cell Prolif*. 2019;52(4):e12631.
18. **Zhang Y**, **Shao J**, **Wang Z**, **et al**. Growth differentiation factor 11 is a protective factor for osteoblastogenesis by targeting PPARgamma. *Gene*. 2015;557(2):209–214.
19. **Flotho A**, **Melchior F**. Sumoylation: a regulatory protein modification in health and disease. *Annu Rev Biochem*. 2013;82:357–385.
20. **Lu L**, **Huang J**, **Zhang X**, **et al**. Changes of temporomandibular joint and semaphorin 4D/Plexin-B1 expression in a mouse model of incisor malocclusion. *J Oral Facial Pain Headache*. 2014;28(1):68–79.
21. **Wang YL**, **Zhang J**, **Zhang M**, **et al**. Cartilage degradation in temporomandibular joint induced by unilateral anterior crossbite prosthesis. *Oral Dis*. 2014;20(3):301–306.
22. **Zhang J**, **Liao L**, **Zhu J**, **et al**. Osteochondral interface stiffening in mandibular condylar osteoarthritis. *J Dent Res*. 2018;97(5):563–570.
23. **Zhang M**, **Wang H**, **Zhang J**, **et al**. Unilateral anterior crossbite induces aberrant mineral deposition in degenerative temporomandibular cartilage in rats. *Osteoarthr Cartil*. 2016;24(5):921–931.
24. **Yang H**, **Zhang M**, **Liu Q**, **et al**. Inhibition of Ihh reverses temporomandibular joint osteoarthritis via a PTH1R signaling dependent mechanism. *Int J Mol Sci*. 2019;20(15):3797.
25. **Wang D**, **Yang H**, **Zhang M**, **et al**. Insulin-like growth factor-1 engaged in the mandibular condylar cartilage degeneration induced by experimental unilateral anterior crossbite. *Arch Oral Biol*. 2019;98:17–25.
26. **Liu Q**, **Yang H-X**, **Wan X-H**, **et al**. Calcium-/calmodulin-dependent protein kinase II in occlusion-induced degenerative cartilage of rat mandibular condyle. *J Oral Rehabil*. 2018;45(6):442–451.
27. **DeFrate LE**, **Kim-Wang SY**, **Englander ZA**, **McNulty AL**. Osteoarthritis year in review 2018: mechanics. *Osteoarthr Cartil*. 2019;27(3):392–400.
28. **Dieppe PA**, **Lohmander LS**. Pathogenesis and management of pain in osteoarthritis. *Lancet*. 2005;365(9463):965–973.
29. **He Z**, **Nie P**, **Lu J**, **et al**. Less mechanical loading attenuates osteoarthritis by reducing cartilage degeneration, subchondral bone remodelling, secondary inflammation, and activation of NLRP3 inflammasome. *Bone Joint Res*. 2020;9(10):731–741.
30. **Lawrence EA**, **Aggleton J**, **van Loon J**, **et al**. Exposure to hypergravity during zebrafish development alters cartilage material properties and strain distribution. *Bone Joint Res*. 2021;10(2):137–148.
31. **Wang XD**, **Zhang JN**, **Gan YH**, **Zhou YH**. Current understanding of pathogenesis and treatment of TMJ osteoarthritis. *J Dent Res*. 2015;94(5):666–673.
32. **Manfredini D**, **Lombardo L**, **Siciliani G**. Temporomandibular disorders and dental occlusion. A systematic review of association studies: end of an era? *J Oral Rehabil*. 2017;44(11):908–923.
33. **Yan F**, **Feng J**, **Yang L**, **Shi C**. The effect induced by alternated mechanical loading on Notch-1 in mandibular condylar cartilage of growing rabbits. *Bone Joint Res*. 2021;10(7):437–444.
34. **Jiang Y**, **Tuan RS**. Origin and function of cartilage stem/progenitor cells in osteoarthritis. *Nat Rev Rheumatol*. 2015;11(4):206–212.
35. **Lippiello L**, **Walsh T**, **Fienhold M**. The association of lipid abnormalities with tissue pathology in human osteoarthritic articular cartilage. *Metab Clin Exp*. 1991;40(6):571–576.
36. **Aspden RM**, **Scheven BA**, **Hutchison JD**. Osteoarthritis as a systemic disorder including stromal cell differentiation and lipid metabolism. *Lancet*. 2001;357(9262):1118–1120.
37. **Francin P-J**, **Abot A**, **Guillaume C**, **et al**. Association between adiponectin and cartilage degradation in human osteoarthritis. *Osteoarthr Cartil*. 2014;22(3):519–526.
38. **Loef M**, **Schoones JW**, **Kloppenburg M**, **Ioan-Facsinay A**. Fatty acids and osteoarthritis: different types, different effects. *Joint Bone Spine*. 2019;86(4):451–458.
39. **Lu B**, **Zhong J**, **Pan J**, **et al**. Gdf11 gene transfer prevents high fat diet-induced obesity and improves metabolic homeostasis in obese and STZ-induced diabetic mice. *J Transl Med*. 2019;17(1):422.
40. **Hernandez S**, **Simoni-Nieves A**, **Gerardo-Ramírez M**, **et al**. GDF11 restricts aberrant lipogenesis and changes in mitochondrial structure and function in human hepatocellular carcinoma cells. *J Cell Physiol*. 2021;236(5):4076–4090.
41. **Li L**, **Wei X**, **Wang D**, **et al**. Positive effects of a young systemic environment and high growth differentiation factor 11 levels on chondrocyte proliferation and cartilage matrix synthesis in old mice. *Arthritis Rheumatol*. 2020;72(7):1123–1133.
42. **Xu X**, **Chu Y**, **Zhang Y**, **et al**. Chondrocyte adipogenic differentiation in softening osteoarthritic cartilage. *J Dent Res*. 2022;101(6):655–663.
43. **Lee JE**, **Schmidt H**, **Lai B**, **Ge K**. Transcriptional and epigenomic regulation of adipogenesis. *Mol Cell Biol*. 2019;39(11):e00601-18.
44. **Lefterova MI**, **Haakonsson AK**, **Lazar MA**, **Mandrup S**. PPARγ and the global map of adipogenesis and beyond. *Trends Endocrinol Metab*. 2014;25(6):293–302.
45. **Cao J**, **Ou G**, **Yang N**, **et al**. Impact of targeted PPARγ disruption on bone remodeling. *Mol Cell Endocrinol*. 2015;410:27–34.
46. **James AW**, **Shen J**, **Khadarian K**, **et al**. Lentiviral delivery of PPARγ shRNA alters the balance of osteogenesis and adipogenesis, improving bone microarchitecture. *Tissue Eng Part A*. 2014;20(19–20):2699–2710.

Author information:

- H. Wang, MS, Attending Physician, State Key Laboratory of Military Stomatology & National Clinical Research Center for Oral Diseases, Department of Medical Rehabilitation, School of Stomatology, The Fourth Military Medical University, Xi'an, China.
- Y. Shi, BSc(Med), Masters student
- F. He, MS, Teaching Assistant
- T. Ye, MS, PhD Student
- S. Yu, PhD, MD, Professor, Chief Physician
- Q. Liu, MD, Attending Physician
- M. Zhang, PhD, MD, Associate Professor, Deputy Chief Physician
  State Key Laboratory of Military Stomatology & National Clinical Research Center for Oral Diseases & Shaanxi International Joint Research Center for Oral Diseases, Department of Oral Anatomy and Physiology and TMD, School of Stomatology, The Fourth Military Medical University, Xi'an, China.
- H. Miao, MD, Associate Professor, State Key Laboratory of Military Stomatology & National Clinical Research Center for Oral Diseases & Shaanxi International Joint Research Center for Oral Diseases, Department of Periodontics, School of Stomatology, The Fourth Military Medical University, Xi'an, China.

Author contributions:

- H. Wang: Conceptualization, Formal analysis, Investigation, Resources, Validation, Writing – original draft.
- Y. Shi: Conceptualization, Formal analysis, Investigation, Methodology, Supervision.
- F. He: Data curation, Formal analysis, Investigation, Methodology, Validation, Writing – original draft.
- T. Ye: Investigation, Methodology, Supervision, Software.
- S. Yu: Data curation, Formal analysis, Funding acquisition, Resources, Software.
- H. Miao: Formal analysis, Funding acquisition, Investigation, Methodology.
- Q. Liu: Data curation, Investigation, Methodology, Resources, Validation, Writing – review & editing.
- M. Zhang: Conceptualization, Funding acquisition, Supervision, Validation, Visualization, Writing – review & editing.

- H. Wang, Y. Shi, and F. He contributed equally to this work.

- Q. Liu and M. Zhang contributed equally to this work.

Funding statement:

- The authors disclose receipt of the following financial or material support for the research, authorship, and/or publication of this article: financial support from the National Natural Science Foundation of China (No. 81700995, Mian Zhang; No. 82001072, Tao Ye; No. 81970953, Shibin Yu) and Natural Science Foundation of Shaanxi Province (2021JM-229, Helin Wang; 2020JQ-453, Tao Ye; and 2021SF-046, Hui Miao).

ICMJE COI statement:

- The authors declare no potential conflicts of interest with respect to the authorship and/or publication of this article.

Acknowledgements:

- We thank Shujing Cai for assistance with establishing the model in rat and preparing histological samples.

Ethical review statement:

- The animal operations were conducted according to the Institutional Animal Care Guidelines and approved by the Laboratory Animal Care & Welfare Committee, School of Stomatology, Fourth Military Medical University (FMMU).

Open access funding

- The authors report that the open access funding for their manuscript was self-funded.

© 2022 Author(s) et al. This is an open-access article distributed under the terms of the Creative Commons Attribution Non-Commercial No Derivatives (CC BY-NC-ND 4.0) licence, which permits the copying and redistribution of the work only, and provided the original author and source are credited. See https://creativecommons.org/licenses/by-nc-nd/4.0/